

# IMAS modelling of First Wall EC heat loads for the ITER re-baseline

Mireille Schneider<sup>1\*</sup>, Jörg Stober<sup>2</sup>, Mélanie Preynas<sup>1</sup>, Sophie Carpentier-Chouchana<sup>1</sup>, Quentin Deliege<sup>1</sup>, Maksim Dubrov<sup>1</sup>, Emanuele Poli<sup>2</sup>, Antoine Sirinelli<sup>1</sup>

<sup>1</sup> ITER Organization, Route de Vinon-sur-Verdon, CS 90 046, 13067 St. Paul-lez-Durance, France

<sup>2</sup> Max-Planck-Institut für Plasmaphysik, Garching, Germany

**Abstract.** This paper describes the modelling work carried out within the ITER Integrated Modelling and Analysis Suite (IMAS) [1] using the TORBEAM wave code [2] to estimate heat loads on the first wall (FW) from operating the Electron Cyclotron (EC) system in various scenarios of the ITER new baseline currently under preparation. These results provide guidance on how to best operate the EC system in terms of polarisation and operating launchers for the various phases of the Research Plan and of a pulse, to limit FW heat loads. Strategies to best protect the FW from EC power losses are also discussed.

## 1 Introduction

Robust operation of the ITER Electron Cyclotron (EC) system, including avoidance of heat loads to in-vessel components, is essential to achieve ITER's mission goals. The main purpose of the system is to provide EC heating (ECH) and current drive (ECCD) to heat and control the plasma to enhance its performance and ensure its stability. ECH/ECCD is essential during the ITER pre-fusion operation phase to provide power for H-mode access, central heating to prevent W accumulation, to control Neoclassical Tearing Modes (NTMs) and, during DT operation, to achieve a high fusion gain and to shape the current profile for hybrid and steady-state scenarios. The EC system will also assist the plasma startup to facilitate breakdown and enhance burn-through. It will also be used for EC Wall Conditioning (ECWC). In all operation phases of the ITER Research Plan (IRP), heat loads on in-vessel components have to be minimised to maximise plasma performance and prevent damage to the machine. For this purpose, a consolidated strategy is being established specifically related to EC heat loads [3]. The IRP is currently being revised as part of a re-baselining proposal [4]. The first operational phase will be performed with an inertially cooled main chamber blanket first wall (FW), while full active cooling of plasma-facing components will be required for the later fusion power operation phases. Excessive EC power losses are problematic in both phases, since the uncooled wall has a limited total energy uptake and the water-cooled first wall components have lower power flux limits. EC heat loads are one of the design drivers for the FW, and it is thus therefore essential to quantify them to proceed with the FW design. This paper describes modelling efforts which have been undertaken to achieve this.

## 2 Re-baseline proposal for the new ITER Research Plan

A key element of the proposed ITER re-baseline is the exchange of FW material from beryllium (Be) to tungsten (W)

which provides a longer erosion lifetime, reduces tritium retention and, as a consequence of the much higher melting temperature, provides greater margins against transient induced material damage [5]. One of the main risk mitigation measures associated with the switch to W is modifying the sharing between IC and EC power in favour of the latter as well as a significant increase in the total installed power with respect to the existing 2016 Baseline to test plasma facing components to Q = 10 relevant loads before DT operation and to demonstrate Q = 10 with ~1 % neutron fluence of the final ITER goal [4]. The new IRP consists of two different phases described in Table 1. The pre-fusion or "Start of Research Operation" (SRO) phase, will be performed with temporary inertially cooled FW panels in H and D plasmas, and aims at commissioning most of the diagnostics, the Plasma Control System (PCS), the Disruption Mitigation System (DMS), the machine protection systems, and Heating and Current Drive systems (H&CD) including 40 MW of ECH and 10 MW of Ion Cyclotron Heating (ICH). This phase should demonstrate L-mode in hydrogen up to the nominal maximum plasma current and toroidal field of  $I_p = 15$  MA and  $B_T = 5.3$  T respectively, and H-mode in deuterium at lower  $I_p$  and  $B_T$  (5-7.5 MA and 2.65 T). In SRO, Ion Cyclotron Wall Conditioning (ICWC) will be developed and tested, and ICH operation will be explored with particular emphasis on the issue of an increased W wall source and possible impact on core W concentration. If IC operation proves to be successful, the system will be upgraded to 20 MW for the fusion power operation phases (named DT-1 and DT-2). For the latter, the temporary FW will be upgraded to the final, actively cooled panel configuration and operation will focus on D, T and DT fuelled plasmas. The EC system will be upgraded to 60 or 67 MW. Two boxes of the Neutral Beam Injection (NBI) will be installed to deliver 33 MW with 870 keV H beams or 1 MeV D beams. In the DT-1 fusion power operation phase, the main goals are to commission the full plant, to demonstrate H-mode at 15 MA, to start the Test Blanket Module (TBM) program, and to demonstrate a fusion gain of Q=10 for 300-500s in DT. For DT-2, an upgrade of the NBI system may be performed with the installation of a third injection box for a total of 50

\* Corresponding author: [mireille.schneider@iter.org](mailto:mireille.schneider@iter.org)

MW NBI. This upgrade would serve the purpose of demonstrating steady-state operation at  $Q=5$ .

**Table 1.** Description of the ITER re-baseline proposal.

	SRO	FPO (DT-1, DT-2)	
First wall	Temporary inertially cooled FW panels	Final actively cooled FW panels for normal heat flux (2 MW/m <sup>2</sup> ) and enhanced heat flux (4.7 MW/m <sup>2</sup> )	
Species	H, D	H, D, DT	DT
H&CD installed power	EC 40 MW IC 10 MW	EC 60-67 MW IC 10-20 MW NB 33 MW	EC 60-67 MW IC 10-20 MW NB 33-50 MW

### 3 The ITER EC system

The detailed status of the ITER EC system for the re-baseline is described in [6]. Table 2 provides a summary. Each Equatorial Launcher (EL) consists of 3 steering mirrors, each hosting 8 beams: Top Steering Mirror (TSM), Middle Steering Mirror (MSM) and Bottom Steering Mirror (BSM). For the first EL, the TSM allows counter-current drive while all other mirrors are oriented for co-current drive. Each Upper Launcher (UL) consists of 2 steering mirrors, each hosting 4 beams: Upper Steering Mirror (USM) and Lower Steering Mirror (LSM). As a consequence of power losses along transmission lines, each beamline, connected to a 1 MW gyrotron, is assumed to deliver 0.83 MW into the plasma. In ITER, the steerable EC mirrors rotate along one axis such that the beams are dominantly poloidally steerable and toroidally almost fixed at  $\sim 25^\circ$  for the EL and  $\sim 20^\circ$  for the UL. In SRO, 48 gyrotrons will be installed for a power delivered to the plasma of up to 40 MW. In the DT phases this will be increased to 72 to 80 gyrotrons, for an injected power of 60 to 67 MW.

**Table 2.** The EC system in the ITER re-baseline proposal.

	SRO	FPO
Equatorial	1 EL 24 beams Up to 20 MW	2 EL 48 beams Up to 40 MW
Upper	3 UL 24 beams Up to 20 MW	3-4 UL 24-32 beams 20-27 MW
Total	48 beams Up to 40 MW (56 beams installed, 48 operated)	72-80 beams Up to 60-67 MW

### 4 Conditions for EC operation in ITER

The optimal operational conditions of the EC system rely on the wave propagation properties. The mechanism to transfer energy from the wave to the electrons involves the resonance between the wave frequency  $\omega$  and the electron cyclotron frequency  $\omega_c = eB/\gamma m_e$ , where  $e$  is the electron charge,  $B$  is the local magnetic field,  $\gamma$  is the relativistic Lorentz factor and  $m_e$  is the rest electron mass. Accounting for the Doppler shift term  $k_{\parallel}v_{\parallel}$  ( $k_{\parallel}$  and  $v_{\parallel}$  being respectively the wave vector and electron velocity components parallel to the magnetic field), the resonance condition is expressed by  $\omega = \omega_c + k_{\parallel}v_{\parallel}$ , characterized by a broadened resonance layer. The wave can only propagate in regions where the density is lower than the so-called cutoff frequency. The X-mode cutoff frequency can

be approximated by  $\omega_R = \sqrt{\left(\frac{eB}{2m_e}\right)^2 + \frac{n_e e^2}{\epsilon_0 m_e} + \frac{eB}{2m_e}}$ , where,  $n_e$  is the electron density and  $\epsilon_0$  is the vacuum permittivity. For

O-mode, the cut-off is at the electron plasma frequency  $\omega_{pe} = \sqrt{\frac{n_e e^2}{\epsilon_0 m_e}}$  which, because it occurs at densities higher than those foreseen for ITER, is never encountered. On the contrary, the X-mode cutoff corresponds to a foreseen operational window (in particular at 5.3 T) as shown in the CMA diagram in Fig. 1. In this figure, the operational path of a beam propagating from the Low Field Side (LFS) to the High Field Side (HFS) is displayed both for the fundamental (at 5.3 T) and second harmonic (at 2.65 T) resonances of the electron cyclotron frequency: at 5.3 T, X1 beams are reflected on the X-mode cutoff, represented by the grey cross in the CMA diagram and by the green curve on the poloidal views of the beam tracing. Note that if the cutoff layer remains relatively close to the cold resonance, partial absorption is expected due to the Doppler shift. The non-absorbed power is reflected leading to heat loads on the LFS. One important feature is that at high density, the X-mode cutoff layer moves to a lower B-field region, i.e. towards the separatrix on the LFS. This feature is important for the protection strategy described in Section 7. In O-mode, the beams are not affected by any cutoff and propagate into the full plasma cross-section to get absorbed. The O1 non-absorbed power leads to direct shine-through losses, creating heat loads on the HFS. At 2.65 T, no cutoff is encountered for either polarisation, hence all losses are expected to be shine-through losses due to reduced plasma density or temperature.

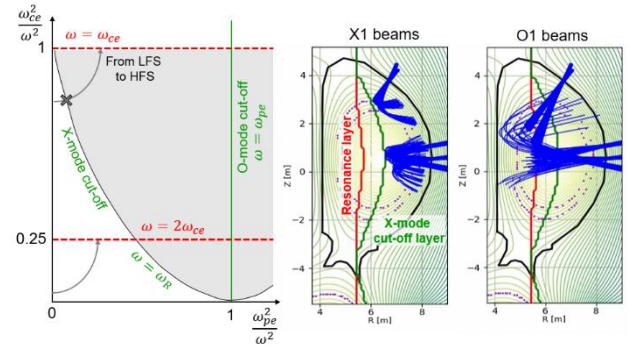


**Fig. 1.** Left figure: CMA diagram for EC beams operated in ITER at the fundamental ( $\omega = \omega_{ce}$ , at 5.3T) and second harmonic ( $\omega = 2\omega_{ce}$ , at 2.65T) resonances. Right figures: beam tracing from TORBEAM wave code at 5.3T in X-mode and O-mode.

These properties of the EC wave allow the most appropriate polarisations at 5.3 T and 2.65 T for the various phases of a discharge to be defined, as summarised in Table 3: for the same harmonic, X-mode absorption is much stronger than O-mode absorption. However, there are two situations for which O-polarisation is favoured: 1) At 2.65 T in H-mode, the high pedestal temperature and density lead to dominant edge parasitic X3 absorption, which prevents central absorption by the EL, see e.g. [7]; 2) At 5.3 T, O-mode is favoured due to the X-mode density cutoff and the associated wave reflection before the cold resonance can be reached. During plasma current ramp-up phase, one can argue that the density cutoff is close enough to the resonance layer, due to the low density, so that X-polarisation should be preferred. The key argument for O-mode operation in this case is that the O1 shine-through losses can be better localised (since they are close to losses in vacuum), whereas the X1 reflection losses depend on the transient density profiles and their location is hard to predict. It is therefore easier to install proper wall protection when operating in O-mode, as described in Section 7.

**Table 3.** Polarisation of the EC system at 5.3 T and 2.65 T for the various phases of a discharge.

B-field	Ramp-up (L-mode)	Flattop in L-mode	Flattop in H-mode
2.65 T	<b>X2:</b> better absorption at low $n_e$ and $T_e$	<b>X2:</b> better absorption, no edge X3	<b>O2:</b> edge parasitic X3
5.3 T	<b>O1:</b> cutoff with X1	<b>O1:</b> cutoff with X1	<b>O1:</b> cutoff with X1

For each of these operational conditions, undesired cross-polarisation can be generated along the transmission lines (including polarisers, mitre bends, corrugated waveguides, etc.). To be conservative, a cross-polarisation of 5% is assumed, leading to the undesired situations described in the Table 3, i.e. lower absorption, edge parasitic X3 or X1 cutoff reflections. The 5% cross-polarisation is an arbitrary value chosen as an envelope to account for polarisation errors on the polariser itself, along the transmission lines, the uncertainties on the magnetic reconstruction and on the algorithm to calculate the optimal polariser angles. The overall results presented in this paper can be rescaled when the total expected cross-polarisation is better quantified.

## 5 The modelling tools

The EC power load study described here is performed using the ITER Integrated Modelling and Analysis Suite IMAS, which consists of predictive and analysis tools developed to support the IRP and prepare ITER operation. IMAS relies on the use of Interface Data Structures (IDS) to represent experimental and simulated data. For the present study, IMAS offers the standard necessary to use existing scenarios from the IMAS scenario database, combined with the geometry of the EC system read from the machine description database. This study uses the TORBEAM beam-tracing code to describe the propagation and absorption of the EC waves in the plasma. In IMAS, TORBEAM reads the *equilibrium* and *core\_profiles* IDS from the scenario database (or from a workflow when used as a component of a transport solver), and the *ec\_launchers* IDS from the machine description database. As an output, it fills the *waves* IDS, written on disk into a local database or transmitted to the rest of the workflow when being used as module of a transport suite.

In addition, specific python tools have been developed to reconstruct Gaussian beams using the information stored in the *waves* IDS, and calculate their immission on the wall surface (represented by rotational poloidal polygons) by projecting beam intensities into the tangential plane at the crossing of the central beam, where they form ellipses, displayed on the projected wall plane (cf. Figs. 2 and 4). The colour of each ellipse represents the beam power density at its centre. Due to the beam Gaussian nature, the intensity at the edge of each ellipse is about one order of magnitude lower.

## 6 Results on EC heat loads

For all the results presented here, the 56 beams corresponding to 4 UL and 1 EL are activated. The second EL is not included since its design is not yet finalised. To help in rescaling the results to the foreseen operational conditions, 1 MW on each beam has been assumed. As a reference and worst-case situation, EC heat loads in vacuum are shown in Fig. 2, with a

scan over the whole poloidal steering range of each beam. The figure also shows a few in-vessel components that may be affected by EC heat loads: the ICH antenna (grey rectangle), the pellet injector exits (magenta points), and the ECH sensors (black points), which are bolometers to measure the EC radiated power. Heat loads from the EL/MSM and EL/BSM mirrors are located on the midplane of the LFS wall, while those from the EL/TSM are deposited on the central column FW panels, due to the fact that the TSM mirror is directed counter-current. The UL produce the highest intensities, up to 200 MW/m<sup>2</sup>, due to their focussed beams (intended to be used for NTM control). Provided that the loads are deposited on a FW panel front surface, due to the high reflectivity of the W wall (~99%), such intensities lead to heat loads of only ~2 MW/m<sup>2</sup>, which are acceptable. Issues occur if such power loads are deposited on gaps between tiles or FW panels, where they get reflected and may eventually deposit on non-tungsten surfaces, leading to potential severe damages. This is why it is important to adapt operation to avoid these gaps.

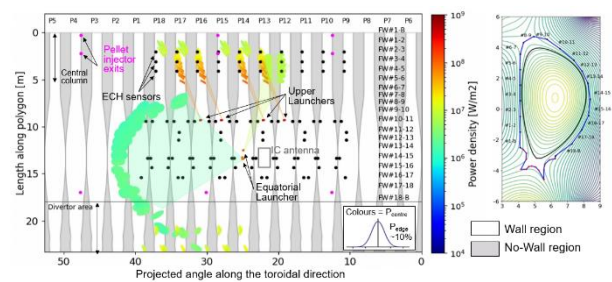


**Fig. 2.** Left: wall projected EC heat loads in vacuum. Right: port numbers and FW segment names linked to poloidal view.

Situations in which the EC system is operated in conditions close to vacuum are, for example, EC-assisted startup (starting without a plasma) and ECWC (low density and very low temperature). In such cases, the plan is to operate only the EL/TSM mirror (i.e. a maximum of 6.7 MW, expected to be sufficient for EC-assist and ECWC), optimal for multiple passes across the midplane. The intensities from the EL/TSM in vacuum are of the order of 5 MW/m<sup>2</sup> (cf. ellipses in port numbers P12 and P13 in Fig. 2) which are reasonable. This figure shows that the IC antenna and the pellet injector exits are safe from EC shine-through losses in such a context. Since the role of ECH sensors is to measure EC heat loads, they should mostly be located where losses are expected, which is the case as shown in Fig. 2.

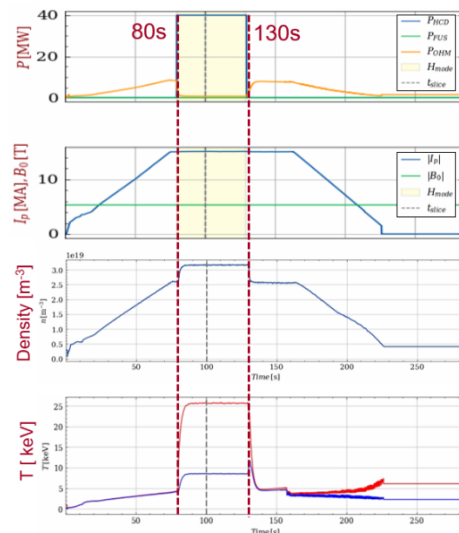


**Fig. 3.** DINA scenario at 15MA/5.3T in H-mode D plasma.



The next step is to examine EC heat loads in the presence of a plasma. For this study, a DINA [8] scenario developed for the re-baseline studies has been selected: a 15 MA/5.3 T D plasma with H-mode in the flattertop (note that for H-mode access in D at 15 MA/5.3 T, power from the IC or NBI systems will need to be added to the 40 MW of EC). This scenario, illustrated in Fig.3, includes 40 MW of EC power applied in the time range [80-130] s and thus only in the flattertop phase (ECH would normally be applied also during the current ramp-up phase to reduce the flux consumption and control the W content level, but this was not the aim of this particular scenario). The resulting heat loads from 5% of X-mode cross-polarisation, estimated using TORBEAM, again for a full poloidal steering scan, are shown in Fig. 4. To facilitate the distinction between EL and UL heat loads, each are displayed separately in the expanded side figures. Comparing these heat loads with those in vacuum from Fig. 2, they show that the majority originate from direct shine-through losses (i.e. their location is similar to that found in vacuum). By elimination, the loads originating from X1 reflections are those dominated by the light green traces (corresponding to intensities  $\sim 20$  MW/m<sup>2</sup>) going from FW18 towards the entry point of each UL. These are time traces which correspond to the cutoff layer moving from the centre of the plasma towards the separatrix when the density increases, as explained in section 4. These results suggest that the UL should not be used for the ramp-up at 5.3T. There are almost no X1 reflection losses from the EL due to that the density remains low enough for this scenario (taken as an extreme at  $\sim 30\%$  of the Greenwald density on the flattertop) such that the cutoff never moves very far from the resonance and the beam path from the EL still reaches high density and temperature region where the power can be absorbed. The situation was different in [9] as the studied scenario was at much higher density, leading to X1 reflections both from the EL and UL. The results in Fig. 4 show that the losses coming from the EL can become significant for the extreme values of the poloidal steering angle (light blue and green area for the most upwards and most downwards injections) but remain in an acceptable range for intermediate steering. Note that the dark blue areas can be ignored since they correspond to the level of ITER Electron Cyclotron Emission (ECE) background radiation expected to be of the order of 100 to 200 kW/m<sup>2</sup>. Heat loads from O-mode polarisation have also been studied and they display a map similar to that in vacuum due to the fact that these are exclusively direct shine-through losses since the O-mode density cutoff is never encountered.

## 7 Potential methods to protect the first wall

Several methods are available to ensure a robust FW protection. The non-absorbed power dissipates in two ways: 1) by being absorbed on the FW, which is potentially harmful and hard to predict after multiple reflections; 2) by being depolarised on the torus curvature, leading to 2<sup>nd</sup> pass absorption for depolarisation from X- to O-mode. The protection strategy should prevent multiple reflections of the beam on the FW since this increases the risk of a gap being impacted. Several methods can be foreseen:

- Against EC shine-through losses, HFS reflectors could be installed on sensitive FW areas to reflect the beam with a specific direction to be absorbed by the plasma for the second pass, see e.g. [10].
- Against X1 reflections: X1 beams will be largely reflected at the outer wall and in particular for the upper launchers they will re-enter the plasma as a focussed beam. The mode mixture of that beam is currently under study, since

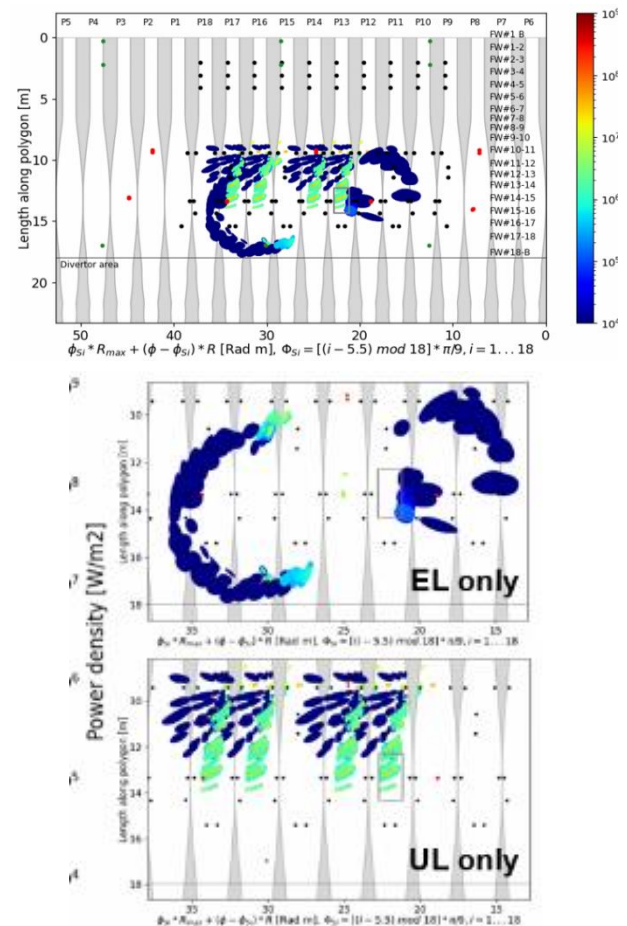


Fig. 4. EC heat loads from 5% of X1 cross-polarisation in the time range [80-115] s for a DINA 15 MA/5.3 T H-mode scenario in D.

its X-mode content will be reflected again from the plasma. Potential counter measures depend on the remaining X-mode content. At high density, the reflective surface is determined since it corresponds to point at which the cutoff layer is at the separatrix. For lower densities, assessing the localisation of FW heat loads from X1 reflections is more tedious and the best strategy is to adapt the operation of the EC system to minimise them.

- To protect the gaps, FW panels might be modified in certain critical areas, though this will be extremely challenging for the final, actively cooled wall.

## 8 Conclusion and prospects

The new ITER baseline includes a significant increase of EC power and this has triggered a re-evaluation of the loads on the first wall associated with EC operation with improved modelling tools. This has identified a series of issues some of which were already present in the 2016 Baseline but not quantified to a high level of accuracy as we have done now. During EC operation, the highest heat loads are expected to be in conditions close to vacuum, i.e. for EC-assisted startup or ECWC. Significant heat loads can also arise from cross-polarisation at 5.3 T when the O-mode is converted into X-mode. If these loads reach first wall panel surfaces, the expected intensities are significant but remain acceptable if the panels are actively cooled or if the deposition occurs during a short period (the exact amount of energy that inertially cooled tiles can sustain is currently under assessment) provided that

adequate protection and operational strategies are implemented. To ensure this, only the EL/TSM mirror, optimised for multiple passes, is planned to be operated for EC-assisted startup and ECWC. To limit shine-through losses, ECH should not be injected at very low plasma densities, so if this is required careful assessment is necessary and careful design may be required. The UL should not be used during the ramp-up since they give the highest heat loads from shine-through losses and X1 reflections and steering angles should be chosen such that beams avoid gaps and sensitive in-vessel components. This protection will be associated with a real-time control strategy managed by the PCS and the machine protection systems, notably the Advanced Protection System and Central Interlock System. The preliminary study presented in this paper aims at providing the basis for the operational and protection strategy and will be refined by extending the number of scenarios foreseen for the re-baseline, including those with ECH in the ramp-up, and covering both SRO and DT phases. To provide more operational flexibility, specific modifications of the first wall (by provision of specific surfaces to decrease X1 reflection losses) and protection for the gaps between first wall panels are being studied. To conclude this study, a map of the vessel should be drawn and applied to all foreseen scenarios to identify which areas are affected by high ECH loads and build an operational strategy or wall design modifications to protect them.

*The views and opinions expressed herein do not necessarily reflect those of the ITER Organization.*

## References

1. F. Imbeaux et al, Nucl. Fusion 55 123006 (2015)
2. E. Poli et al., Comp. Phys. Comm. 225, 36 (2018)
3. M. Preynas et al, this workshop
4. A. Loarte et al., “Initial evaluations in support of the new ITER baseline and Research Plan”, ITR-24-004 (2024) <https://www.iter.org/technical-reports>
5. R. A. Pitts et al., to be submitted to Nucl. Mater. and Energy
6. N. Casal et al, this workshop
7. M. Schneider et al, Nucl. Fusion 61 126058 (2021)
8. R.R. Khayrutdinov and V.E. Lukash, J. Comp. Phys. 107 106 (1993)
9. J. Stober et al, 49th EPS conference, 3-7 July, Bordeaux, France (2023)
10. M. Schubert et al, EPJ Web of Conferences 203, 02009 (2019)